Research Article

Graft Copolymerization of Acrylonitrile and Ethyl Acrylate onto *Pinus Roxburghii* Wood Surface Enhanced Physicochemical Properties and Antibacterial Activity

Gaurav Sharma [iD],[1,2] **Amit Kumar** [iD],[1,2] **Mu. Naushad** [iD],[3] **Fahad A. Al-Misned,**[4]
Hamed A. El-Serehy,[4] **Ayman A. Ghfar,**[3] **Kulwant Rai Sharma,**[5] **Chuanling Si** [iD],[6]
and Florian J. Stadler [iD][1]

[1]*College of Materials Science and Engineering, Shenzhen Key Laboratory of Polymer Science and Technology, Guangdong Research Center for Interfacial Engineering of Functional Materials, Nanshan District Key Laboratory for Biopolymers and Safety Evaluation, Shenzhen University, Shenzhen 518060, China*
[2]*School of Chemistry, Shoolini University, Solan 173212, Himachal Pradesh, India*
[3]*Department of Chemistry, College of Science, King Saud University, Riyadh, Saudi Arabia*
[4]*Department of Zoology, College of Science, King Saud University, Riyadh, Saudi Arabia*
[5]*Dr. Yashwant Singh Parmar University of Horticulture and Forestry, Nauni 173230, Solan, Himachal Pradesh, India*
[6]*Tianjin Key Laboratory of Pulp and Paper, Tianjin University of Science and Technology, Tianjin 300457, China*

Correspondence should be addressed to Gaurav Sharma; gaurav8777@gmail.com and Mu. Naushad; naushadksu@rediffmail.com

As a natural and the most abundant material, wood was used as a scaffold for the grafting of acrylonitrile (AN) and ethyl acrylate (EA) to develop a novel grafted wood. Thus, chemical modification of the wood was carried out by means of grafting. It is clear from the characterization techniques (FTIR, SEM, and XRD) that grafting of acrylonitrile (AN) and ethyl acrylate (EA) was successfully performed on the *Pinus roxburghii* wood. Monomer and initiator concentration, temperature, time, and pH parameters have been varied to obtain the maximum percent grafting yield. A significant influence was observed on the physicochemical properties, morphological structure, and bacterial resistant nature after the graft copolymerization of AN + EA on the raw wood. This approach of grafting of wood would lead to the construction of a new class of materials with better properties and will also promote innovative consumption of renewable wood.

1. Introduction

Nature offers a number of biological materials that could be utilized for the preparation of new materials with desirable properties beneficial for one or other applications. Recent studies have revealed that bio-based materials from marine organisms, insects, plants tissues, etc., have immense applications in diverse fields such as medicine and industries [1–3]. The diverse synthetic materials have been extensively used for environmental detoxification as adsorbents and photocatalysts [4–7]. But their expensive and toxic nature hinders their utilization at large scale. The natural bio-based material can be a possible alternative for their substitution, if modified effectively for desired application. These materials have been successfully used for remediation of heavy metals and organic wastes [8–12]. Precisely, wood-based products show better properties and have excellent features of easy penetrability and reactivity, which are fundamentally different from other materials [13–18]. A number of techniques, such as grafting, radiation, and chemical modification, have been used for improving the properties of such materials [19–21].

The gristly nature of wood has made it an important biomaterial. The stability and long-lasting nature of the wood composites are due to the presence of cellulose, hemicellulose, and lignin. Its cellular structure has made it as strong as steel [22–26]. It also helps in the transportation of fluids throughout the plant body. Scientists are working on increasing the stability and hardness of the wood composites so as to replace the traditionally used steel and other lavishing non-ecofriendly materials [27–31].

The presence of hydroxyl ions in the wood increases its rate of degradation. Scientists have found a best solution to overcome this problem [32–34]. Chemical modification helps in reducing the combustibility of the wood and also helps in improving its behavior under undesirable environmental conditions. They actually chemically modify the wood so as to make the hydroxyl ions unavailable for the degradation process [35].

Chemical modification is based on the supposition that there should be a direct relation between induced functionality and its related property, thus making it fit for specific application [36]. Due to chemically selective nature of induced functionality, the undesired reaction cannot take place on the chemically modified wood surface. These surfaces are even resistant to termites decay and help in improving the dimensional stability [24, 37, 38].

Ethyl acrylate (EA) and acrylonitrile (AN) were chosen as potential monomers for grafting onto raw *Pinus* wood because of their unique functionalities and diverse properties. Ethyl acrylate is an acrylic monomer explored for production of diversity of polymers and copolymers as part of various commercially utilized goods. EA was studied for improvisation of physical properties of natural and synthetic polymers; the properties of polymers obtained from natural resources, as wood cellulose and fibres were successfully modified using EA. The ethyl acrylate/alkyl methacrylate graft copolymerization efficiency and conversion into amylose were investigated [39]. Similarly, grafting of hydroxyl methacrylates/ethyl acrylate onto amylopectin was performed to fabricate biocompatible materials [40]. The cellulosic fibres were functionalized by graft copolymerization of acrylonitrile/ethyl acrylate and were investigated for moisture absorption nature and chemical resistance under different environments [41]. On the other hand, acrylonitrile contains a vinyl group linked to the nitrile group. This vital monomer was investigated for the production of plastics, as polyacrylonitrile. The chitosan has been modified with acrylonitrile; the obtained materials showed promising antibacterial properties [42]. When cellulose was grafted with the acrylonitrile monomer, it was transformed into a decent adsorbent with better adsorption capacity for removal of chromium ions [43].

In the present paper, we demonstrated that how grafting on the wood can change the properties of the *Pinus roxburghii* wood. We also demonstrated how the functionality of acrylonitrile (AN) and ethyl acrylate (EA) can be grafted onto the wood and the obtained functional wood material possesses the novel profiles. This chemically modified wood was used for the physiochemical studies, and its antibacterial properties were also studied in detail.

2. Materials and Methods

2.1. Materials and Reagents. Wood strips of *Pinus roxburghii* were provided by Dr. Yashwant Singh Parmar, University of Horticulture and Forestry, Nauni (Solan), Himachal Pradesh, India. After keeping the collected wood strips of *Pinus roxburghii* at room temperature for 2-3 days, they were immersed into water for one day at room temperature. The wood strips were then taken out and dried at room temperature. Acrylonitrile (AN) was purchased from Loba Chemie Ltd., ammonium ceric nitrate (CAN) from Chem Light Laboratories Pvt. Ltd., ethyl acrylate (EA) from Central Drug House (P) Ltd., and nitric acid (NA) from Loba Chemie Ltd.

2.2. Preexperimental Condition. The wood strips used here were of the following dimension: 200 mm × 20 mm × 2 mm: longitudinal × tangential × radial. They were then presoaked for one complete day and then dried to obtain a constant weight. The dried wood strips were then subjected to solvent extraction for delignification (in benzene/acetone/methanol in 4 : 1 : 1 by v/v) for 24 h. Strips were again dried at 105°C for 5 h and then moved to a desiccator to be cooled at room temperature and then weighed on the balance.

2.2.1. Acrylonitrile and Ethyl Acrylate Grafting onto Raw Pinus Wood. The acrylonitrile and ethyl acrylate grafting was carried out on the surface of *Pinus* wood by means of free-radical polymerization. Optimal grafting yield was achieved by varying parameters such as time, temperature, monomer concentration, and initiator concentration.

2.3. Physiochemical Behavior of Pinus-Raw and Pinus-G-(AN/EA)

2.3.1. Swelling Behavior. Swelling behavior of *pinus-raw* and *pinus-g-(AN/EA)* in different solvents (phosphate buffer with pH 2, phosphate buffer with pH 9, benzene, DMW, and NaCl) was studied. For this purpose, the samples, i.e., *pinus-raw* and *pinus-g-(AN/EA)*, were immersed in 100 mL of each solvent, and then, change in the weight was noted at different time intervals (20–1440 min). Then, the excess solvent was removed by gently pressing the samples in the folds of the filter paper. The final weight of the sample was noted. Percent swelling was calculated by using the following formula [44]:

$$\%\text{swelling} = \frac{W_f - W_i}{W_i} \times 100, \tag{1}$$

where W_f = final weight of wood strips and W_i = initial weight of wood strips.

2.3.2. Chemical Resistivity Study. The study of chemical resistance was performed by plunging samples of *pinus-raw* and *pinus-g-(AN/EA) wood* of known weight in different solvents of different strengths. The chemical resistivity of the raw and modified wood was considered in context of percent weight loss. The change in weight was calculated at different

time intervals (20–1440 min). After each interval, the samples were taken out and weight of each sample was noted after removing the excess solution by gently pressing them within the folds of a filter paper. Percent weight loss was obtained as follows:

$$\%weightloss = \frac{W_1 - W_2}{W_1} \times 100, \qquad (2)$$

where $W_1 =$ initial weight of the sample and $W_2 =$ final weight of the sample.

2.4. Characterization Techniques.
Fourier transform infrared (FTIR) spectra of *pinus-raw* and *pinus-g-(AN/EA)* were recorded by using a PerkinElmer Spectrum 400 FT-IR/FT-FIR spectrophotometer using KBr pellets and was analyzed in the range of 400–4000 cm^{-1}. The surface morphologies of the *pinus-raw* and *pinus-g-(AN/EA)* samples were studied by using a Quant-250 scanning electron microscope (SEM). The image resolution was noted at 50X and 500X. Before focusing the electron beam on the samples, these samples were coated with gold suspension so that they become conducting [45]. X-ray diffraction (XRD) is an analytical procedure used for generalizing nature of *pinus-raw* and *pinus-g-(AN/EA)* wood. Each sample was finely powdered and homogeneously mixed before exposing to X-rays. These homogenized samples were uncovered to X-rays from all possible planes. The angle of scattering of the diffracted beam was measured in context to the incident beam of X-rays and relative intensity was found [46]. The radiation used was Cu K-α^{-1}, whereas nickel metal is used as the beta filter.

2.5. Applications

2.5.1. Antibacterial Activity and Lead Adsorption.
Nutrient agar medium was prepared by adding 2.8 grams of nutrient agar in 100 mL of distilled water which was poured into four Petri dishes [47]. All the materials were autoclaved (i.e., 4 swaps, tips, nutrient medium) for 45 min, and 25 mL of this autoclaved medium was poured into each plate. This medium was placed in the laminar for 15 min so as to solidify it. *E. coli* was then swapped on the medium with the help of a micropipette. The wood pieces of *pinus-raw* and *pinus-g-(AN/EA)* of sizes 2 mm, 4 mm, 6 mm, and 8 mm were added to the solidified nutrient agar medium. These strips were then placed in the incubator for 72 h at 37°C, and the results were noted. To investigate the adsorption behavior of *pinus-g-(AN/EA)* wood, the known amount of it was placed in lead ion solution of known concentration for a specific time interval. The concentration of lead ions was recorded before and after adsorption experiments [48].

3. Result

3.1. Grafting Mechanism.
The complete mechanism for the grafting of EA and AN on the *Pinus* raw wood has been presented in Scheme 1. Cerium ions of CAN generate free ra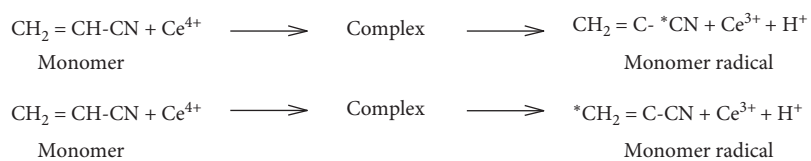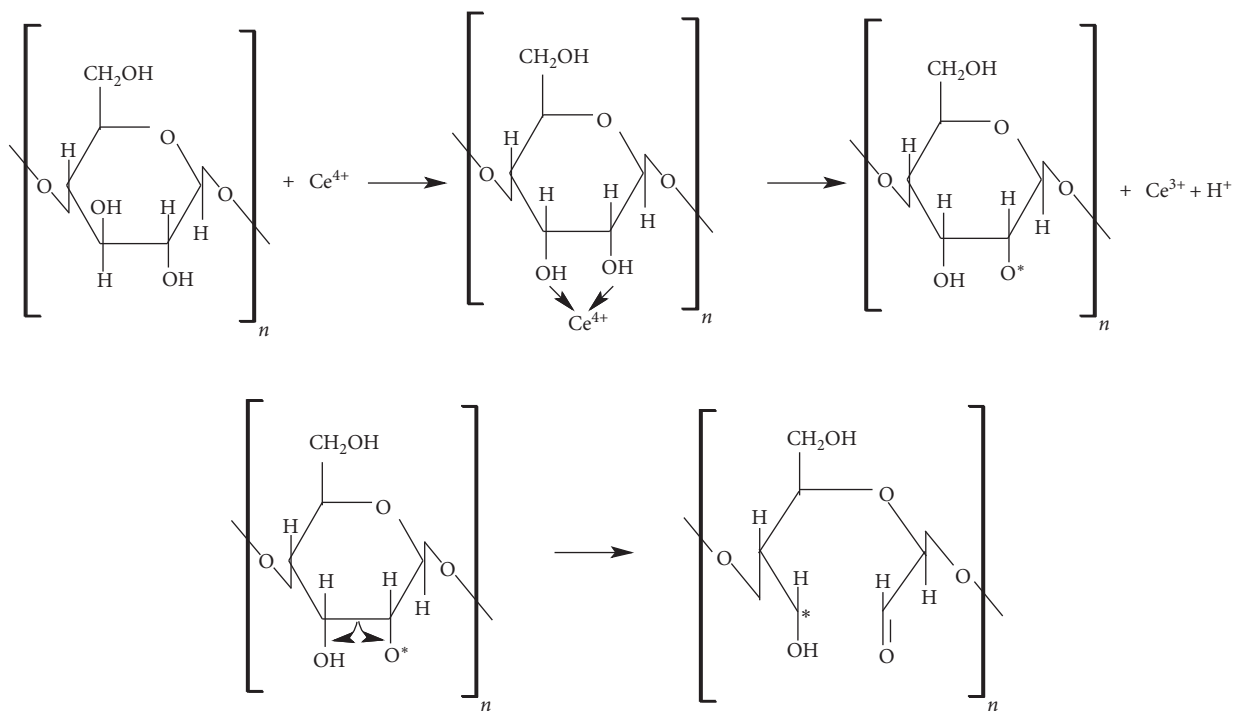dicals by their reaction with wood, acrylonitrile (AN), and ethyl acrylate (EA) which leads to grafting of monomers onto the surface of *Pinus* raw wood. The maximum percentage grafting (85.34%) for raw *Pinus roxburghii* wood was achieved at optimized parameters.

3.2. Characterization.
Figure 1 demonstrates the FTIR spectrum of *pinus-raw* and *pinus-g-(AN/EA)*. The broad peaks in the region of 3400–3397 cm^{-1} were due to the existence of hydrogen bonded –OH stretching of cellulose [49]. A peak at 2919.9 cm^{-1} is for C-H stretching vibration, whereas a peak at 2117.18 cm^{-1} is due to the –OH stretching of absorbed moisture. A peak at 1640.8 cm^{-1} is assigned to the H–O–H bending of the absorbed water molecule and C–H deformation of lignin. A characteristic peak at 1505.8 cm^{-1} was observed for lignin aromatic ring vibration and stretching. The peaks present at 1159.3 cm^{-1} for –C–O–C and 1050.3 cm^{-1} for –C–O stretching in xylan side substituent and lignin aromatic C–O stretching. The peak observed at 898 cm^{-1} was due to β-glycosidic linkage and at 607.11 cm^{-1} was due to out-of-plane –OH bending [44, 50, 51]. In case of *pinus-g-(AN/EA)*, additional peaks were found at 2241 cm^{-1} for the –C≡N group of acrylonitrile and at 1733 cm^{-1} for the carbonyl group (>C=O) of α- and β-unsaturated esters present in the ethyl acrylate.

The variations in topography and morphology of wood surfaces were considered by SEM. Figures 2(a) (*pinus-raw*) and Figures 2(b) (*pinus-g-(AN/EA)*) show the change in morphologies of raw and modified wood. It is observed that the surface of *pinus-g-(AN/EA)* is highly rough as compared to *pinus-raw*, which is credited to high graft density [52]. The hole size of *pinus-raw* is large in comparison with *pinus-g-(AN/EA)* which becomes small due to attachment of monomers and as a result, adhesion power is increased. Figures 3(a) and 3(b) show the patterns of XRD of *pinus-raw* and *pinus-g-(AN/EA)*, respectively. The peaks are observed at 2 θ values of 22.74° and 18.42°. It shows the large difference in peak intensities, signifying variations in the crystallinity of cellulose [53]. The values given in Table 1 reveal that upon grafting, both crystallinity index and percent crystallinity values have reduced. The value of crystallinity index detected for grafted cellulose is lower which suggests that there may be disorientation of cellulose crystals and poor crystal lattice order in it due to incorporation of (AN + EA) chains in the cellulose backbone.
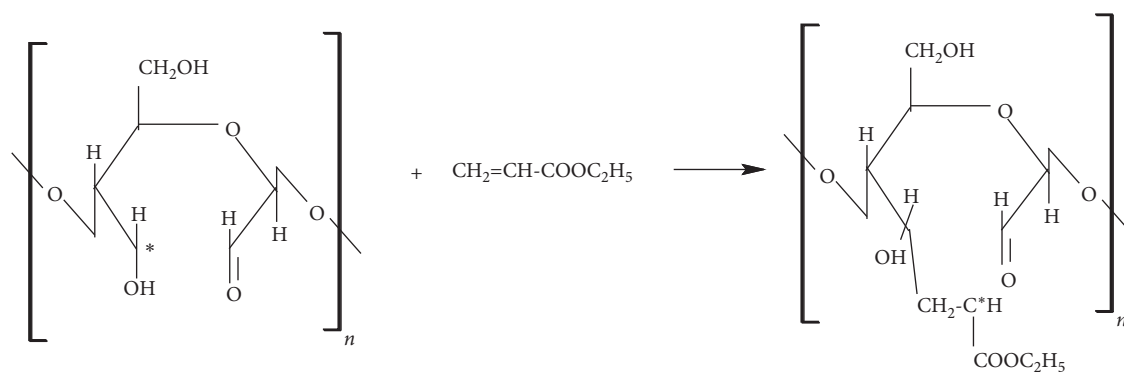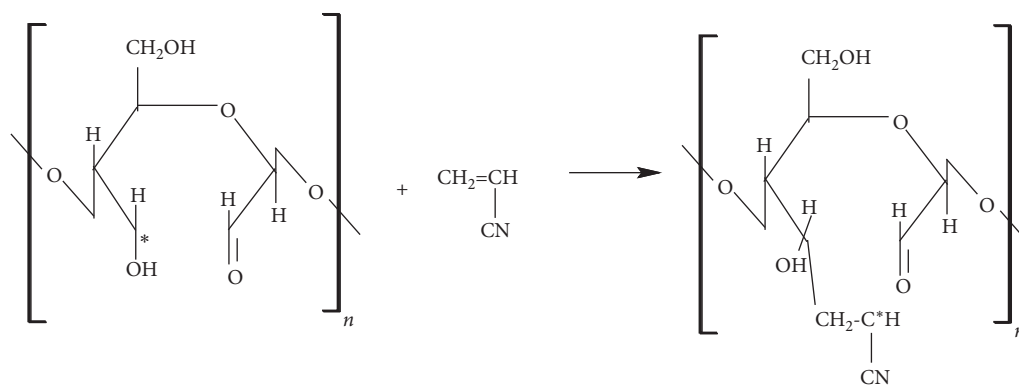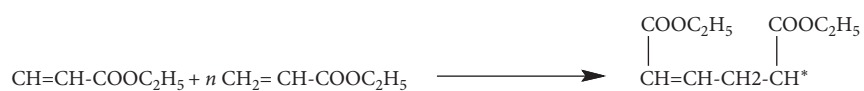
3.3. Reaction Parameters Optimization for Graft Copolymerization of AN + EA onto Pinus-Raw Wood Strips

3.3.1. Reaction Temperature Effect.
The reaction temperature effect was studied at diverse temperatures (35°C, 45°C, 55°C, 65°C, and 75°C). Figure 4(a) shows that with initial increase in temperature, percent graft yield increases up to 74.3% for *Pinus* which is the optimal value observed at 65°C and decreases with further increase in reaction temperature. This variation of percent graft yield with the increase of temperature is due to an upsurge in the diffusion rate of

$$CH_2 = CH\text{-}CN + Ce^{4+} \longrightarrow \text{Complex} \longrightarrow CH_2 = C\text{-}{}^*CN + Ce^{3+} + H^+$$
Monomer   Monomer radical

$$CH_2 = CH\text{-}CN + Ce^{4+} \longrightarrow \text{Complex} \longrightarrow {}^*CH_2 = C\text{-}CN + Ce^{3+} + H^+$$
Monomer   Monomer radical

(a)

Scheme 1: Continued.

$CH_2=CH-CN + {}^*CH=CH-COOC_2H_5 \longrightarrow$

$$
\begin{array}{c}
H \\
| \\
C=CH_2-CH=C-COOC_2H_5 \\
| \\
CN
\end{array}
$$

Binary radical

$CH_2=CH-COOC_2H_5 + CH_2=C-CN \longrightarrow$

$$
\begin{array}{c}
CH_2 \\
|| \\
CH-CH2-C-CN \\
| \\
COOC_2H_5
\end{array}
$$

$$
\begin{array}{cc}
CH_2= C^* + & n\ CH_2 = CH \\
| & | \\
CN & CN
\end{array}
\longrightarrow
\begin{array}{cc}
CH_2= C - CH_2 - {}^*CH \\
| \qquad\quad | \\
CN \qquad\ CN
\end{array}
$$

$$
CH=CH-COOC_2H_5 + n\ CH_2= CH-COOC_2H_5 \longrightarrow
\begin{array}{cc}
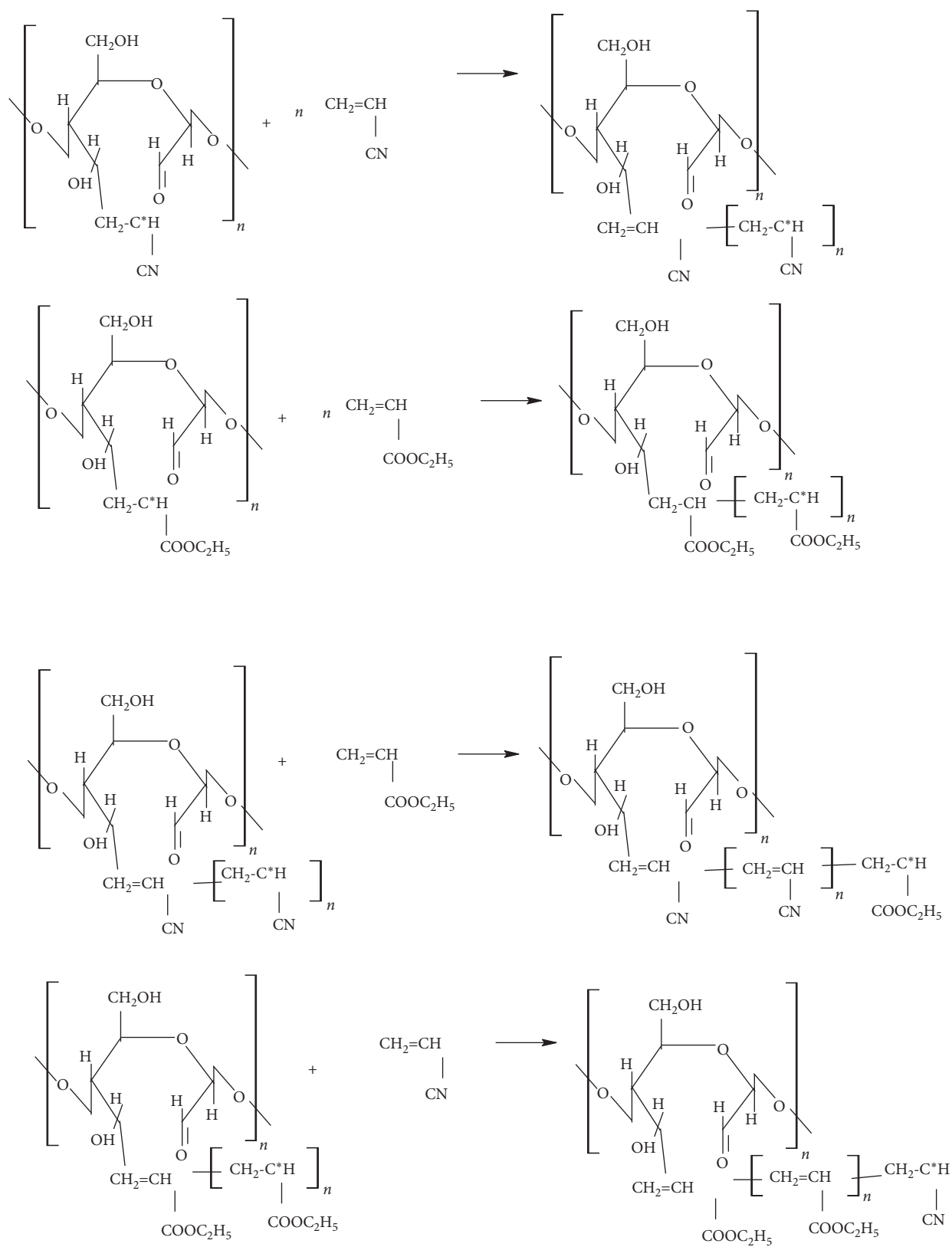COOC_2H_5 & COOC_2H_5 \\
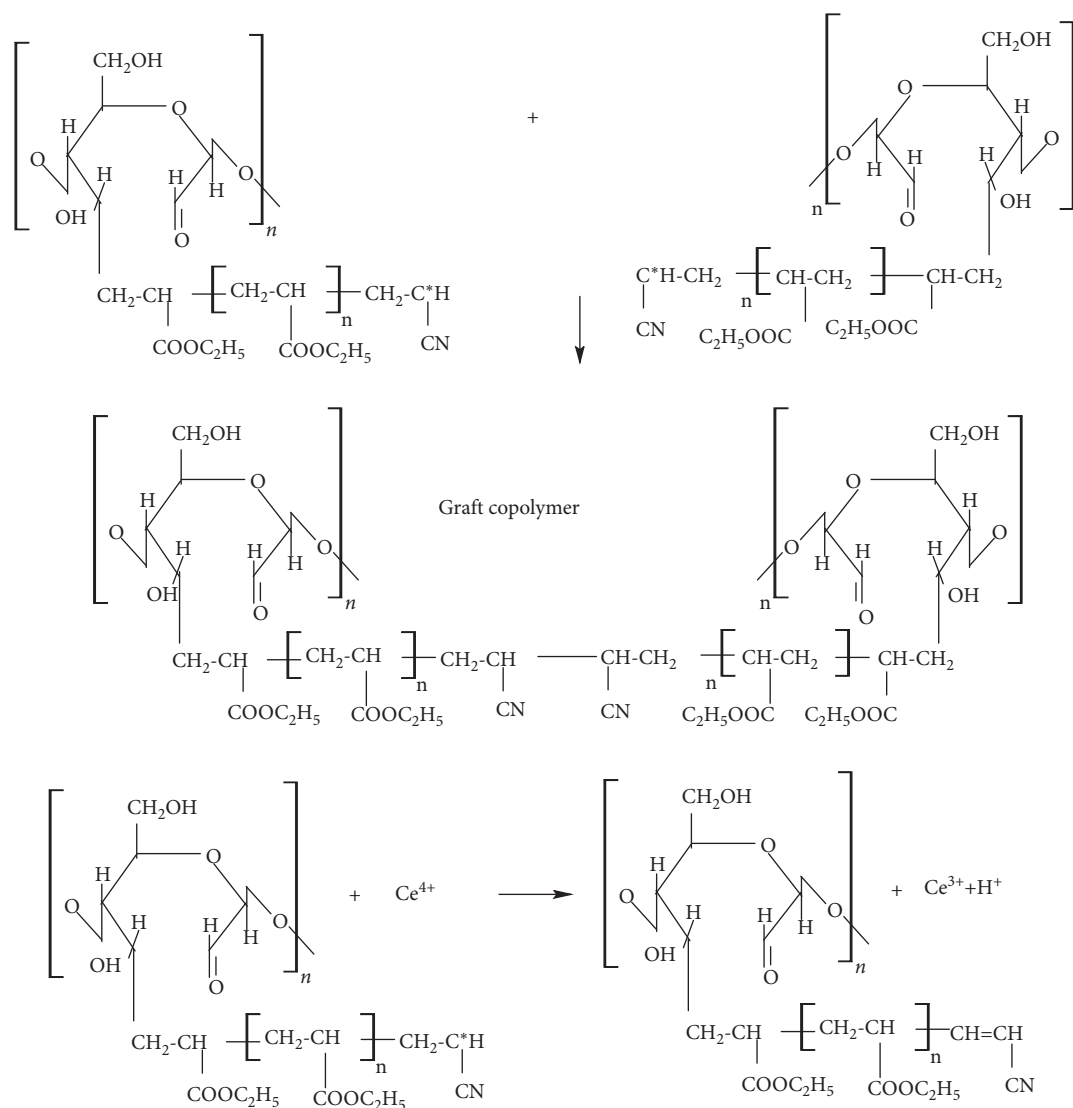| & | \\
CH=CH-CH2-CH^*
\end{array}
$$
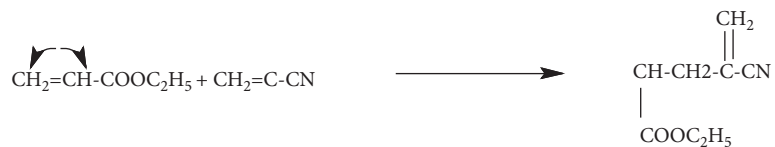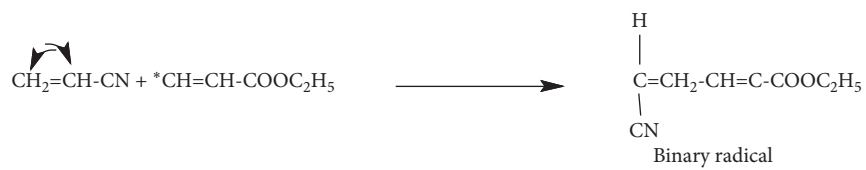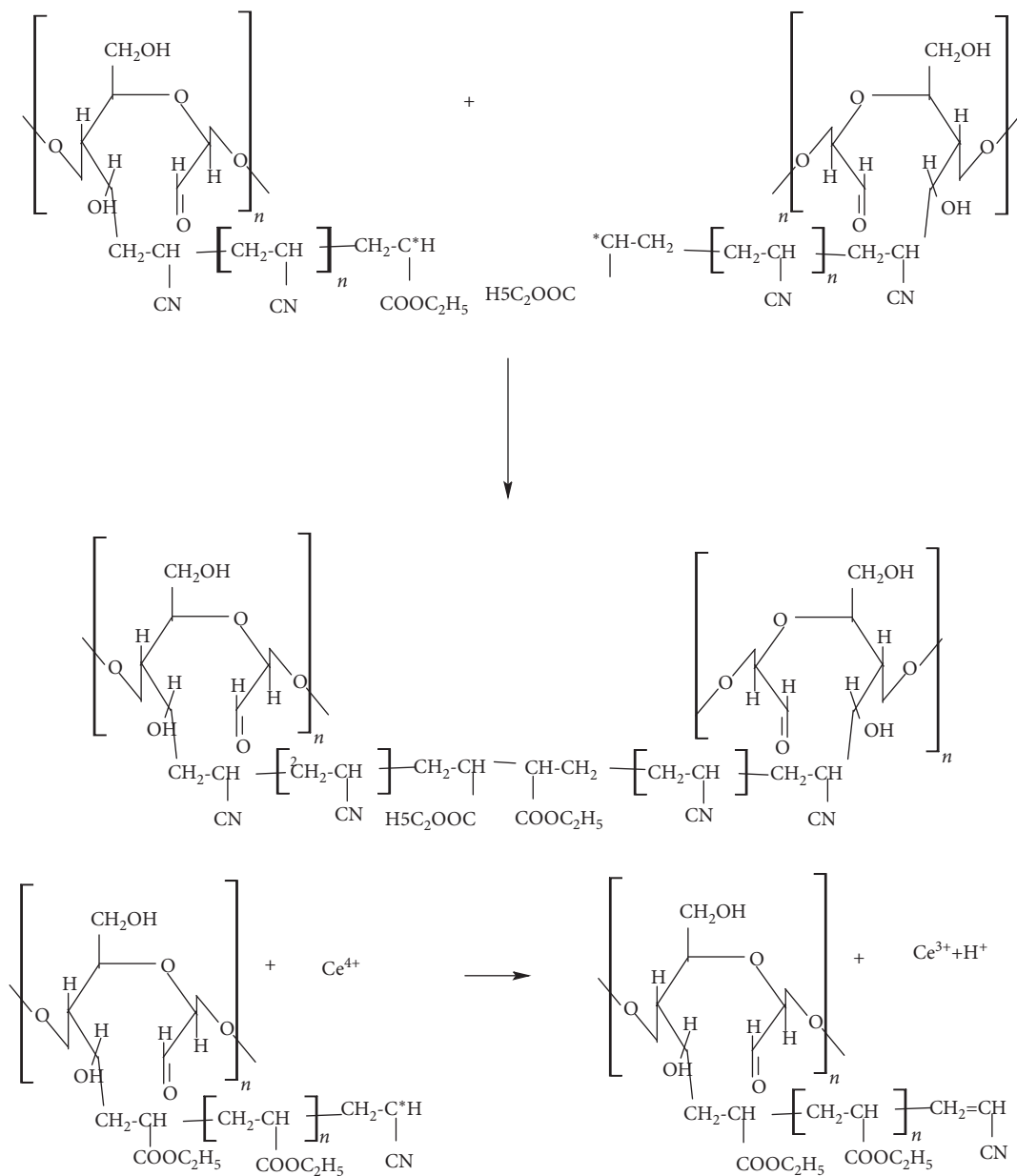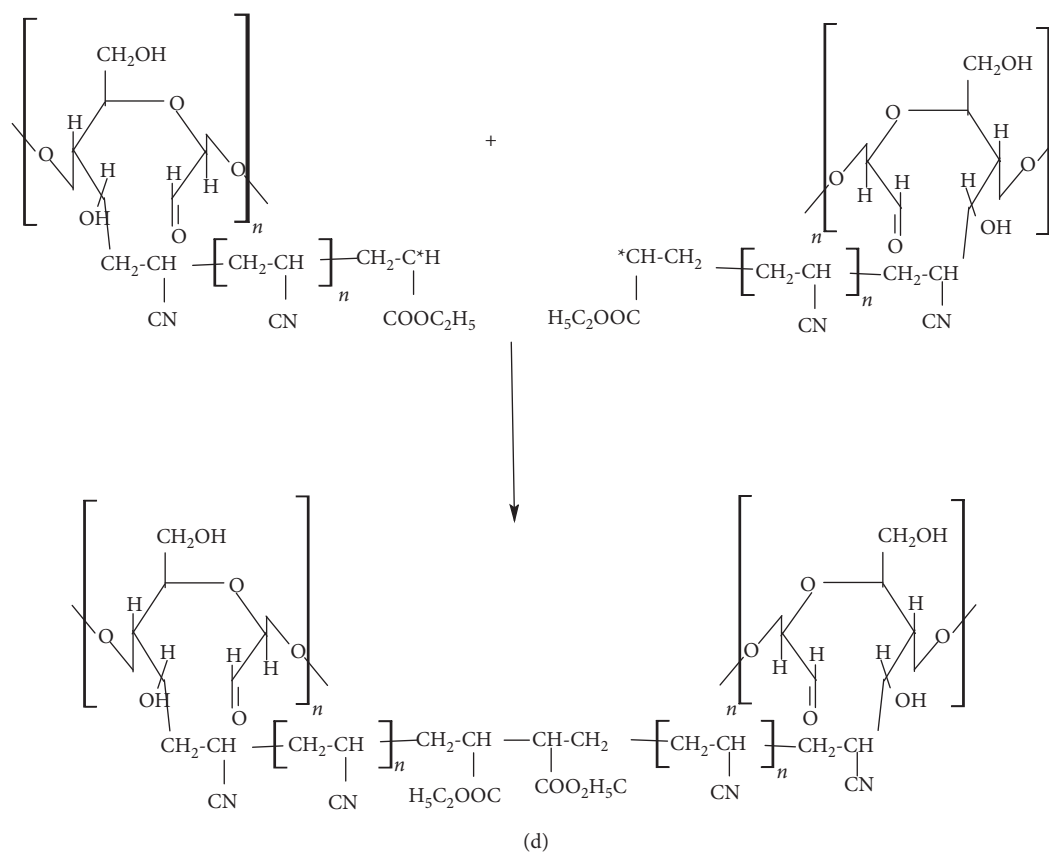
(b)

Scheme 1: Continued.

(c)

Scheme 1: Continued.

SCHEME 1: Continued.

Scheme 1: Continued.

Scheme 1: The proposed mechanism for grafting. (a) Radical generation. (b) Chain initiation. (c) Chain propagation. (d) Chain termination.
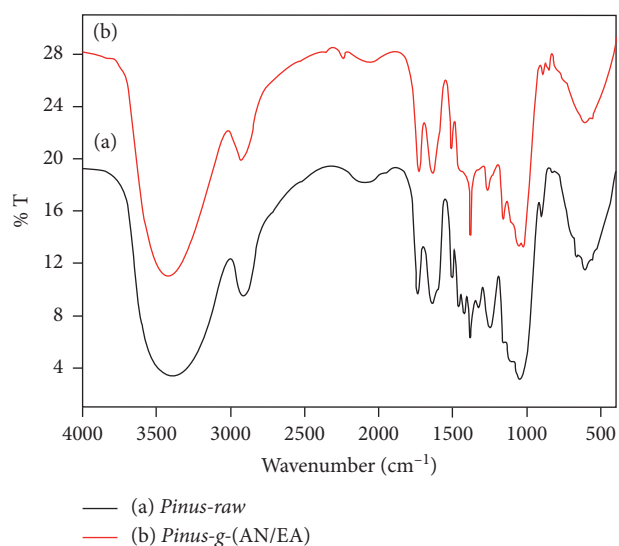

Figure 1: FTIR spectrum of (a) pinus-raw and (b) pinus-g-(AN/EA).

monomer molecules from reaction mixture onto wood backbone, resulting in the high percent graft yield. There is decrease in percent yield with further increase in temperature, which may be due to the upsurge in the rate of chain transfer or termination reactions between monomer molecules and grafted chain. Also, there is a combination of free

monomer radicals, which leads to decreased percent graft yield with the rise in temperature.

3.3.2. Reaction Time Effect. The reaction time effect on the graft copolymerization of AN + EA onto *Pinus-raw* wood was observed after 1 h, 2 h, 3 h, 4 h, and 5 h. Graft yield increases with the initial increase in time, reaches optimal value at 3 h, and then decreases with further upsurge in reaction time as shown in Figure 4(b). The variation of percent graft yield with time is elucidated on the basis that as the reaction time upsurges, more and more radicals move onto the backbone and increases the graft yield [54]. Most of the active sites present on the backbone are occupied by radicals after reaching the optimum value. Now, if there is further upsurge in reaction time, the formation of homopolymer dominates over the graft copolymerization.

3.3.3. Initiator Concentration Effect. Ceric ions generate CAN complexes with carbon chains on the wood surface backbone to produce active sites. Ceric ions also generate free radicals in the monomer and increase free ion concentration and percent grafting as the concentration of the initiator increases. The percent grafting was studied at different initiator concentrations (5%, 7%, 12%, 15%, and 20%) as shown in Figure 4(c). After reaching the optimal value of 7%, the graft yield decreases with further upsurge in
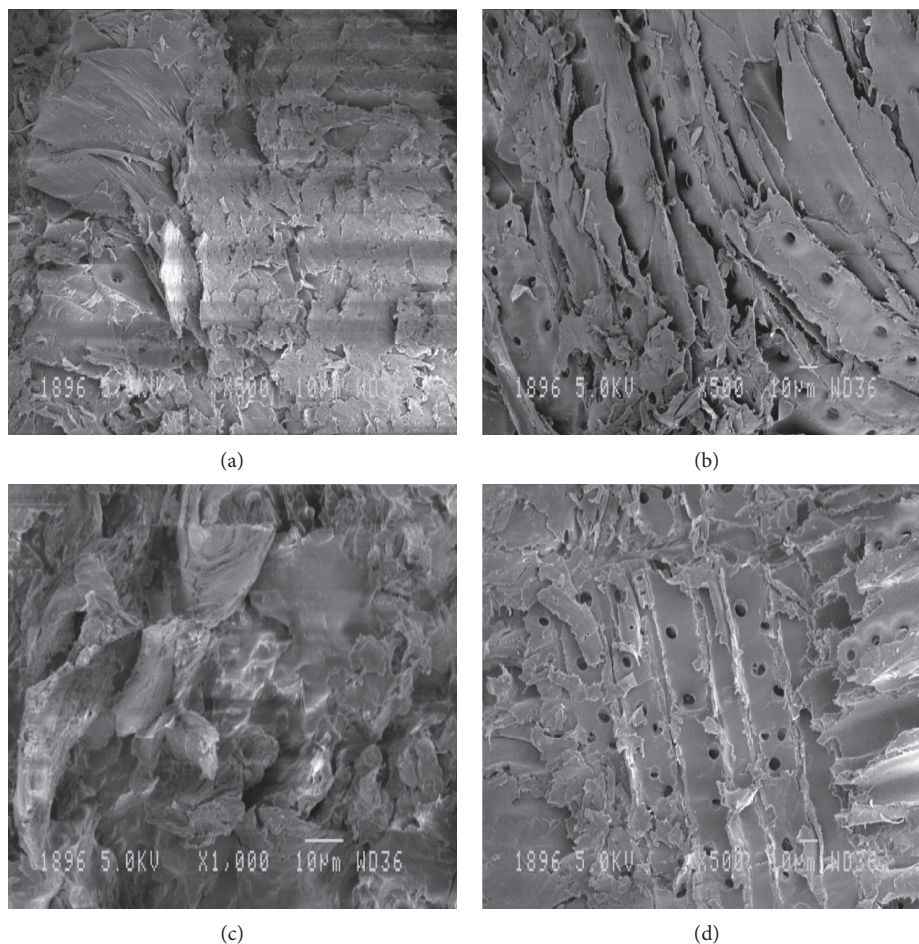
(a)

(b)

(c)

(d)

FIGURE 2: SEM image of (a) *pinus-raw* and (b) *pinus-g-(*AN/EA*)*.

(a)

(b)
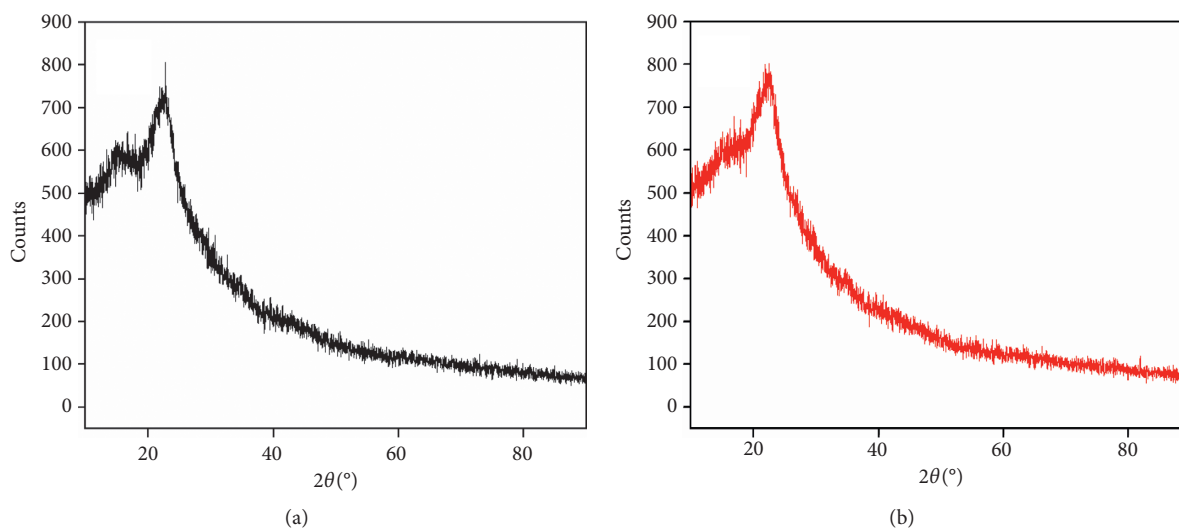
FIGURE 3: XRD image of (a) *pinus-raw* and (b) *pinus-g-(*AN/EA*)*.

initiator concentration [55]. This is because chain termination reactions dominate the graft copolymerization with increase in initiator concentration, which leads to premature decay of the monomer radicals.

3.3.4. Monomer Concentration Effect. The percent graft yield varies with the monomer concentration (Figure 4(d)) and reaches the optimum value, i.e., 73.3% (for *Pinus-raw*), at monomer concentration $0.2\,M\ EA + 0.2\,M\ AN$ and then

TABLE 1: Crystallinity index and % crystallinity of *pinus-raw* and *pinus-g-(AN/EA)*.

Sample	Crystallinity index	% crystallinity
Pinus-raw	0.26	58
Pinus-g-(AN/EA)	0.20	55

decreases with further change in monomer concentration as shown in Figure 4(d). The monomer concentration effect may be elucidated on the basis of more homopolymer formation at other concentrations. As the monomer concentration reaches the optimal value, graft copolymerization dominates the homopolymerization, leading to rise in graft yield [56].

3.3.5. Reaction pH Effect.

The percent graft yield was studied at different pH values (2, 5, 7, 9, and 14). The percent graft yield increases with decrease in pH, i.e., with increase in acidic condition and decrease in basic condition, as evaluated from Figure 4(e). The maximum percent graft yield has been found at pH 2. Further increase in pH caused the decrease in the graft yield. This could be due to premature termination of polymerization reaction at basic pH.

3.4. Physicochemical Properties

3.4.1. Swelling Behavior.

Different solvents demonstrate unlike trends in the swelling behavior of *pinus-raw* and p*inus-g-(AN/EA)*, as revealed in Figures 5(a) and 5(b). The maximum swelling is observed in phosphate buffer at pH 2 in both raw as well as grafted wood. In case of raw wood, the phosphate buffer solution at pH 2 shows the maximum swelling of 178% due to the presence of polar –OH groups which shows greater affinity towards the water molecules. But in case of grafted wood, the -OH groups are gradually replaced by (AN + EA) chains and thus the number of –OH groups decreases which results in decrease in percent swelling of 70% for grafted wood as compared to raw wood. A considerable amount of swelling occurs in case of benzene (61%) for grafted wood as the affinity of (AN + EA) towards benzene is high but still it is less in comparison to raw wood (170%). In grafted woods, there is presence of alkyl groups in (AN + EA) chains which are hydrophobic in nature and having strong affinity towards nonpolar solvents like benzene. The trend of swelling in different solvents is given as follows:

Raw wood strips (*pinus-raw*): buffer phosphate of pH 2 > DMW > buffer phosphate of pH9 > NaCl > benzene

Grafted wood strips (*pinus-g-(AN/EA)*): buffer phosphate of pH 2 > benzene > NaCl > buffer phosphate of pH9 > DMW

In general, overall, the swelling % decreases in the grafted wood as compared to raw wood in every solvent, thus revealing that chemical modification of pinus wood helped in reducing its affinity for adsorption of solvents.

3.4.2. Chemical Resistivity Study.

The chemical resistance behavior of *pinus-raw* and *pinus-g-(AN/EA)* was studied in acids and bases of different strengths. It has been observed that the effect of different acids and bases on the modified wood, i.e., *pinus-g-(AN/EA)*, is less as compared to raw wood strips, i.e., *pinus-raw*. Figures 6(a) and 6(b) demonstrate the percent weight loss for *pinus-raw* and *pinus-g-(AN/EA)* wood. The % weight loss was about 26% for *pinus-raw* in 5 M HNO_3 + 5 M HCl as compared to *pinus-g-(AN/EA)*, where it is only 15%. It was observed that after the grafting, the acid-base tolerance of *Pinus* wood increased . The detailed results are presented in Figure 6. Hence, the covering of wood surface with (AN + EA) chains after grafting enhances the stability of wood against acid and base attacks. The acid and base resistance for *pinus-g-(AN/EA)* wood can be attributed to two reasons, i.e., the presence of AN + EA covering on wood surface provides an external layer that protects the internal wood structure by preventing the entrance of acid and bases into wood pores and the other reason may be that grafting replaces the more reactive hydroxyl groups with –C=O and –C≡N which increase resistance of *pinus-g-(AN/EA)* wood.

4. Applications

4.1. Antibacterial Activity.

The antibacterial activity was studied with the help of the disc diffusion method which shows the high resistance of *pinus-g-(AN/EA)* against bacteria as compared to *pinus-raw*. In this activity, there is formation of an inhibition zone around the raw and modified wood. A large zone is formed around the wood of *pinus-g-(AN/EA)*. Due to the resistive nature of AN + EA, it inhibits the growth of *E. coli* around it. However, there is a formation of small zone around the *pinus-raw* and it cannot inhibit the growth of *E. coli* around it as no such protective covering is present due to which *E. coli* grow easily around the wood strips. The maximum zone of inhibition was observed around 8 mm size of wood strips, i.e., 21 mm for *pinus-g-(AN/EA)*. The detailed results are shown in Figure 7.

4.2. Wastewater Treatment.

Due to rapid and continual industrialization over past decades, the accretion of heavy metals in water and soils, discharged from various industries (such as smelting, mining, electroplating and agricultural activities), has become a serious environment problem [57]. We have utilized *pinus-g-(AN/EA)* as an adsorbent for the removal of highly toxic Pb(II) metal ion from the aqueous medium. For this study, 50 mg of *pinus-g-(AN/EA)* was shaken with 100 mL solution of 50 ppm of Pb(II) metal ion. It was noticed that 86.5% of Pb(II) metal ion was adsorbed within 2 h which showed the high adsorption efficiency of *pinus-g-(AN/EA)* towards Pb(II) metal ion. The results
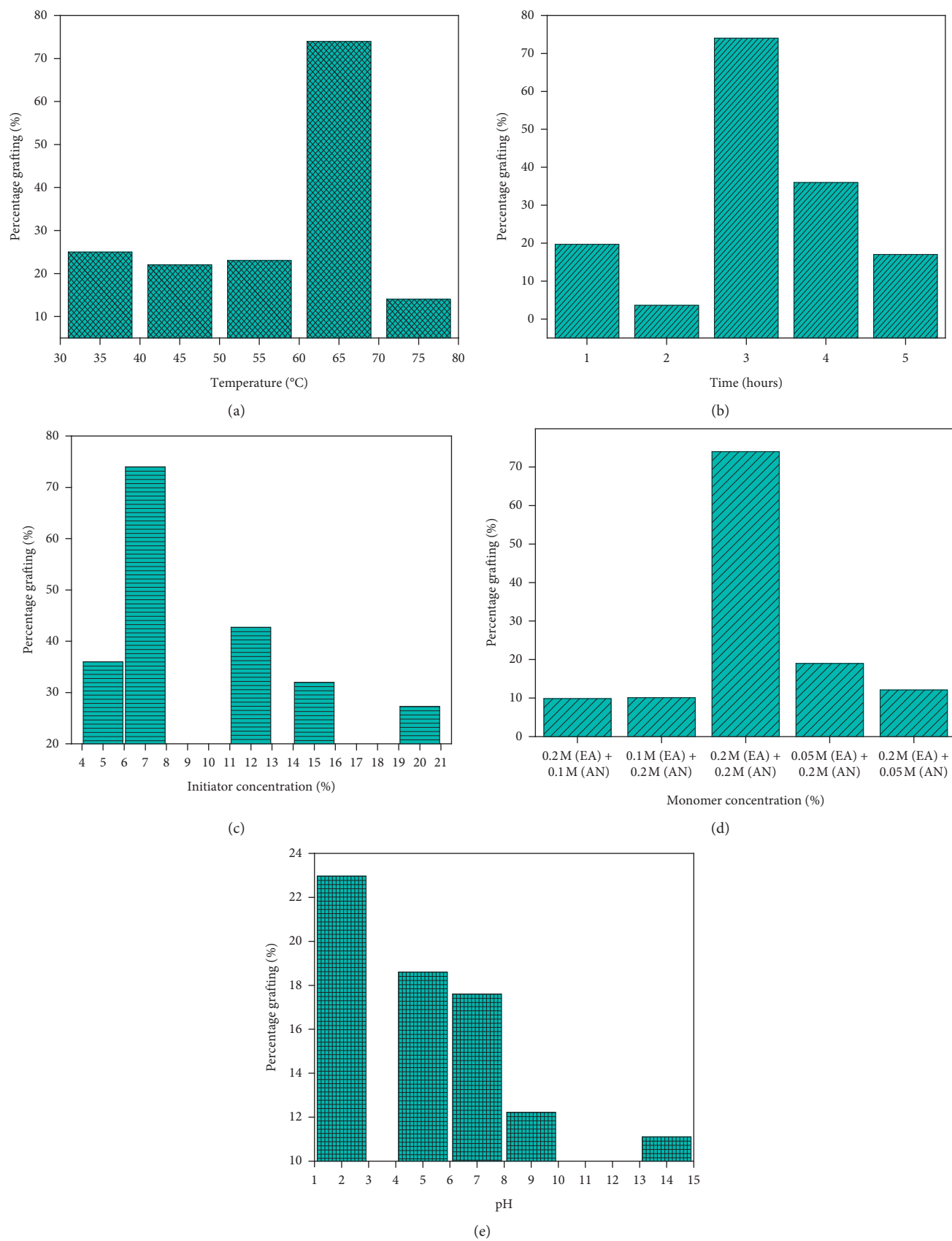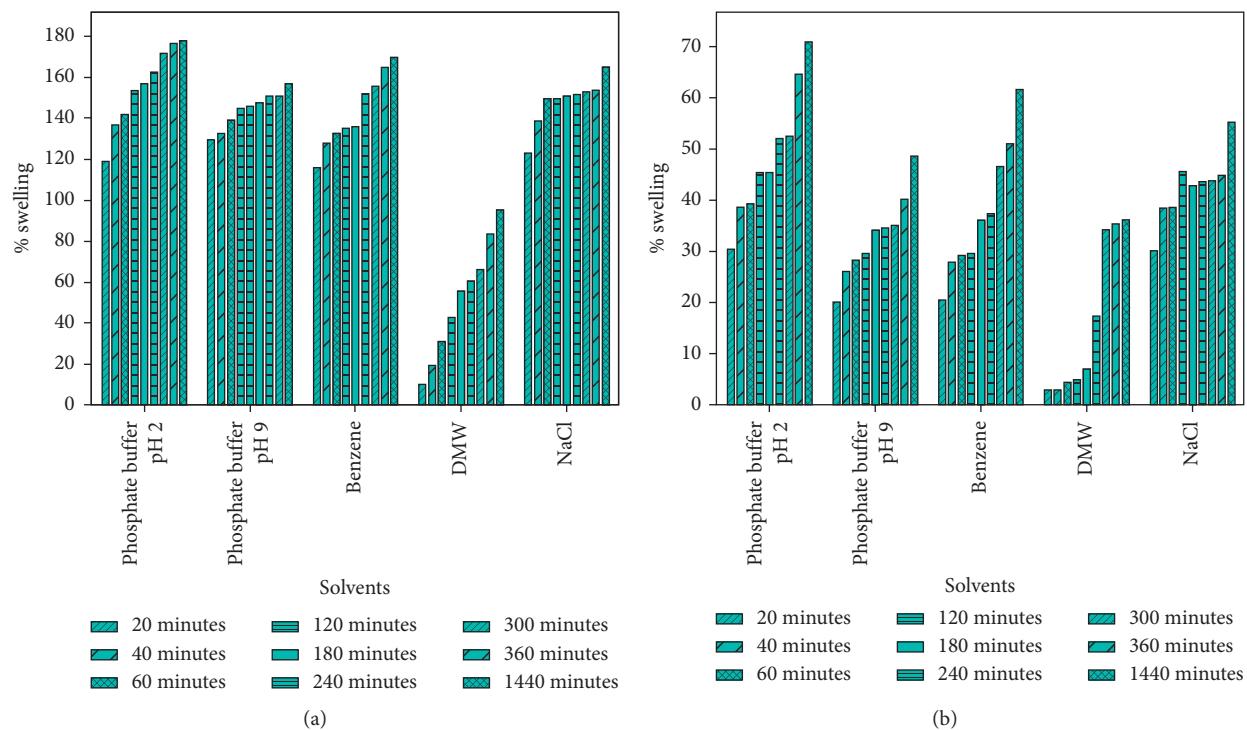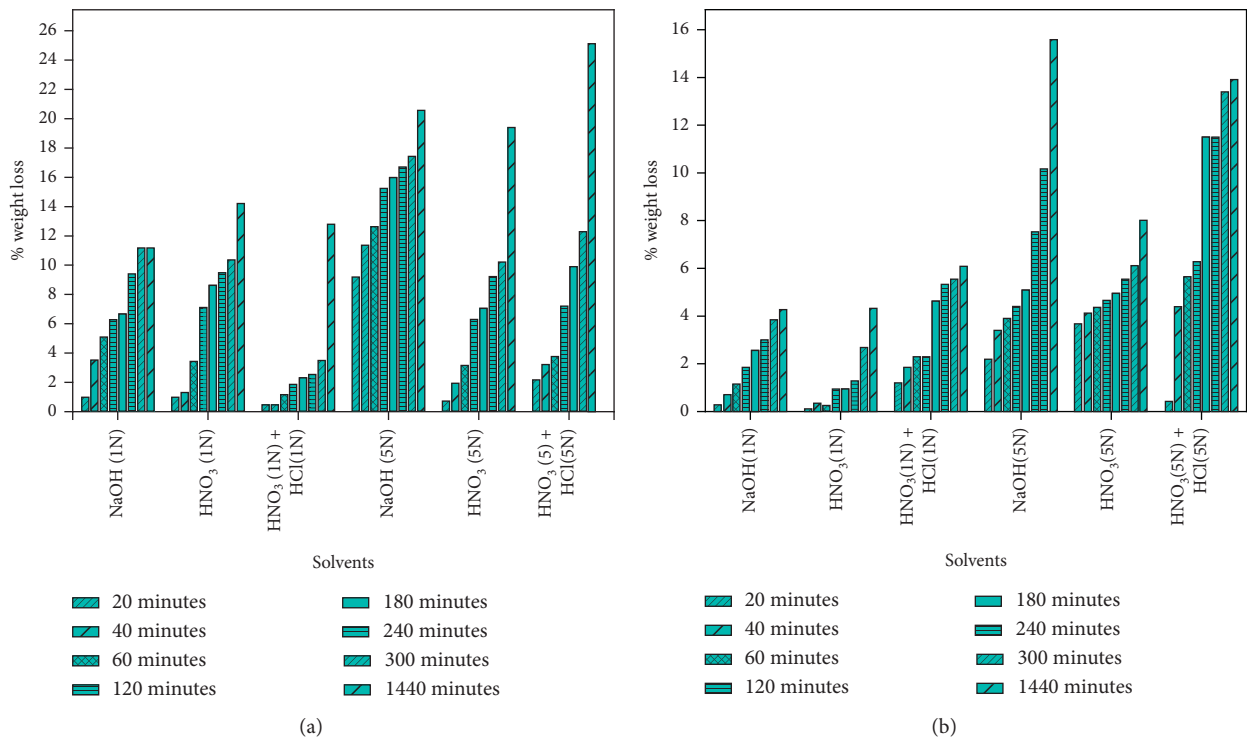
Figure 4: Optimization of reaction parameter for *pinus-g-(AN/EA)*. (a) Temperature. (b) Time. (c) Initiator concentration. (d) Monomer concentration. (e) pH.

Figure 5: Swelling studies for (a) *pinus-raw* and (b) *pinus-g-(AN/EA)*.

Figure 6: Chemical resistivity of (a) *pinus-raw* and (b) *pinus-g-(AN/EA)*.
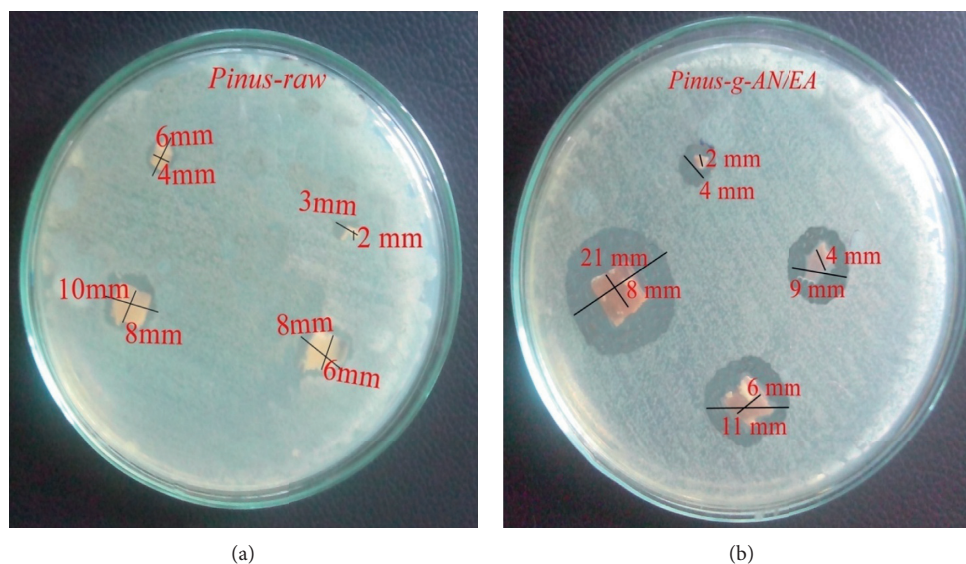
(a)

(b)

FIGURE 7: Antibacterial activity images of (a) *pinus-raw* and (b) *pinus-g-(AN/EA)*.

demonstrated that *pinus-g-(AN/EA)* was a good and economical adsorbent and had broad application prospects.

5. Conclusion

To obtain the maximum grafting (% yield: 85.34) for *Pinus roxburghii,* different reaction parameters were optimized, i.e., initiator amount at 7%, monomer concentration of 0.2 M AN + 0.2 M EA, reaction time of 3 h, and temperature of 65°C. The desired functionality was revealed by the FTIR spectrum which showed the characteristics peaks at $2241 \, cm^{-1}$ for –C≡N group of acrylonitrile and $1733 \, cm^{-1}$ for the carbonyl group (>C=O). Thus, modification in physicochemical properties of raw wood can be obtained by graft copolymerization of a binary monomer mixture of AN + EA. *Pinus-g-(AN/EA)* wood showed more resistance to attack of acids and bases, inhibited the activity of bacteria, and also showed less swelling. *Pinus-g-(AN/EA)* was also used as an adsorbent for the removal of highly toxic Pb(II) metal ions from the aqueous medium, and it removed 86.5% Pb(II) within 2 h. So, *Pinus-g-(AN/EA)* was a good and economical adsorbent and had broad application prospects.

Data Availability

No data were used to support this study.

Conflicts of Interest

All authors declare that there are no conflicts of interest.

Acknowledgments

References

[1] M. Naushad, T. Ahamad, G. Sharma et al., "Synthesis and characterization of a new starch/SnO₂ nanocomposite for efficient adsorption of toxic Hg²⁺ metal ion," *Chemical Engineering Journal*, vol. 300, pp. 306–316, 2016.

[2] Y. Zhou, S. Cao, C. Xi et al., "A novel Fe₃O₄/graphene oxide/citrus peel-derived bio-char based nanocomposite with enhanced adsorption affinity and sensitivity of ciprofloxacin and sparfloxacin," *Bioresource Technology*, vol. 292, p. 121951, 2019.

[3] G. Sharma, B. Thakur, M. Naushad et al., "Applications of nanocomposite hydrogels for biomedical engineering and environmental protection," *Environmental Chemistry Letters*, vol. 16, no. 1, pp. 113–146, 2018.

[4] X. Liu, J. Wu, S. Zhang et al., "Amidoxime-functionalized hollow carbon spheres for efficient removal of uranium from wastewater," *ACS Sustainable Chemistry & Engineering*, vol. 7, no. 12, pp. 10800–10807, 2019.

[5] H. Chen, J. Li, D. Shao, X. Ren, and X. Wang, "Poly(acrylic acid) grafted multiwall carbon nanotubes by plasma techniques for Co(II) removal from aqueous solution," *Chemical Engineering Journal*, vol. 210, pp. 475–481, 2012.

[6] G. Sharma, D. Pathania, and M. Naushad, "Preparation, characterization, and ion exchange behavior of nanocomposite polyaniline zirconium(IV) selenotungstophosphate for the separation of toxic metal ions," *Ionics*, vol. 21, no. 4, pp. 1045–1055, 2014.

[7] I. Mironyuk, T. Tatarchuk, M. Naushad, H. Vasylyeva, and I. Mykytyn, "Highly efficient adsorption of strontium ions by carbonated mesoporous TiO₂," *Journal of Molecular Liquids*, vol. 285, pp. 742–753, 2019.

[8] J. Li, Z. Guo, S. Zhang, and X. Wang, "Enrich and seal radionuclides in magnetic agarose microspheres," *Chemical Engineering Journal*, vol. 172, no. 2-3, pp. 892–897, 2011.

[9] J. Sun, X. Liu, F. Zhang et al., "Insight into the mechanism of adsorption of phenol and resorcinol on activated carbons with different oxidation degrees," *Colloids and Surfaces A: Physicochemical and Engineering Aspects*, vol. 563, pp. 22–30, 2019.

[10] J. Yi, Z. Huo, X. Tan et al., "Plasma-facilitated modification of pumpkin vine-based biochar and its application for efficient

elimination of uranyl from aqueous solution," *Plasma Science and Technology*, vol. 21, Article ID 095502, 2019.

[11] M. Naushad, G. Sharma, and Z. A. Alothman, "Photo-degradation of toxic dye using gum Arabic-crosslinked-poly(acrylamide)/Ni(OH)$_2$/FeOOH nanocomposites hydro-gel," *Journal of Cleaner Production*, vol. 241, Article ID 118263, 2019.

[12] M. Naushad, G. Sharma, A. Kumar et al., "Efficient removal of toxic phosphate anions from aqueous environment using pectin based quaternary amino anion exchanger," *International Journal of Biological Macromolecules*, vol. 106, pp. 1–10, 2018.

[13] A. R. Studart, "Biological and bioinspired composites with spatially tunable heterogeneous architectures," *Advanced Functional Materials*, vol. 23, no. 36, pp. 4423–4436, 2013.

[14] D. W. Behnken, "Estimation of copolymer reactivity ratios: an example of nonlinear estimation," *Journal of Polymer Science Part A: General Papers*, vol. 2, no. 2, pp. 645–668, 1964.

[15] W. J. Chappas and J. Silverman, "The effect of acid on the radiation-induced grafting of styrene to polyethylene," *Radiation Physics and Chemistry (1997)*, vol. 14, pp. 847–852, 1979.

[16] P.-Y. Chen, J. McKittrick, and M. A. Meyers, "Biological materials: functional adaptations and bioinspired designs," *Progress in Materials Science*, vol. 57, no. 8, pp. 1492–1704, 2012.

[17] T. Darmanin and F. Guittard, "Superhydrophobic and superoleophobic properties in nature," *Materials Today*, vol. 18, no. 5, pp. 273–285, 2015.

[18] P. W. Tidwell and G. A. Mortimer, "An improved method of calculating copolymerization reactivity ratios," *Journal of Polymer Science Part A: General Papers*, vol. 3, no. 1, pp. 369–387, 1965.

[19] E. Cabane, T. Keplinger, T. Künniger, V. Merk, and I. Burgert, "Functional lignocellulosic materials prepared by ATRP from a wood scaffold," *Scientific Reports*, vol. 6, p. 31287, 2016.

[20] G. Sharma, M. Naushad, A. Kumar et al., "Efficient removal of coomassie brilliant blue R-250 dye using starch/poly(alginic acid-cl-acrylamide) nanohydrogel," *Process Safety and Environmental Protection*, vol. 109, pp. 301–310, 2017.

[21] G. Sharma, M. Naushad, D. Pathania, A. Mittal, and G. E. El-desoky, "Modification of *Hibiscus cannabinus* fiber by graft copolymerization: application for dye removal," *Desalination and Water Treatment*, vol. 54, no. 11, pp. 3114–3121, 2015.

[22] K. Yu, T. Fan, S. Lou, and D. Zhang, "Biomimetic optical materials: integration of nature's design for manipulation of light," *Progress in Materials Science*, vol. 58, no. 6, pp. 825–873, 2013.

[23] E. S. Lintz and T. R. Scheibel, "Dragline, egg stalk and byssus: a comparison of outstanding protein fibers and their potential for developing new materials," *Advanced Functional Materials*, vol. 23, no. 36, pp. 4467–4482, 2013.

[24] T. Speck and I. Burgert, "Plant stems: functional design and mechanics," *Annual Review of Materials Research*, vol. 41, no. 1, pp. 169–193, 2011.

[25] C. Etienne, K. Tobias, M. Vivian, H. Philipp, and B. Ingo, "Renewable and functional wood materials by grafting po-lymerization within cell walls," *ChemSusChem*, vol. 7, no. 4, pp. 1020–1025, 2014.

[26] U. G. K. Wegst, H. Bai, E. Saiz, A. P. Tomsia, and R. O. Ritchie, "Bioinspired structural materials," *Nature Materials*, vol. 14, no. 1, pp. 23–36, 2014.

[27] I. Burgert, E. Cabane, C. Zollfrank, and L. Berglund, "Bio-inspired functional wood-based materials—hybrids and

[28] R. R. Devi, I. Ali, and T. K. Maji, "Chemical modification of rubber wood with styrene in combination with a crosslinker: effect on dimensional stability and strength property," *Bioresource Technology*, vol. 88, no. 3, pp. 185–188, 2003.

[29] T. Keplinger, E. Cabane, M. Chanana et al., "A versatile strategy for grafting polymers to wood cell walls," *Acta Biomaterialia*, vol. 11, pp. 256–263, 2015.

[30] Y. Xie, Q. Fu, Q. Wang, Z. Xiao, and H. Militz, "Effects of chemical modification on the mechanical properties of wood," *European Journal of Wood and Wood Products*, vol. 71, no. 4, pp. 401–416, 2013.

[31] M. B. Agustin, F. Nakatsubo, and H. Yano, "Improving the thermal stability of wood-based cellulose by esterification," *Carbohydrate Polymers*, vol. 192, pp. 28–36, 2018.

[32] W. E. Hillis, "High temperature and chemical effects on wood stability," *Wood Science and Technology*, vol. 18, no. 4, pp. 281–293, 1984.

[33] C. B. Vick and R. M. Rowell, "Adhesive bonding of acetylated wood," *International Journal of Adhesion and Adhesives*, vol. 10, no. 4, pp. 263–272, 1990.

[34] E. T. Engelund, L. G. Thygesen, S. Svensson, and C. A. S. Hill, "A critical discussion of the physics of wood-water interactions," *Wood Science and Technology*, vol. 47, no. 1, pp. 141–161, 2013.

[35] R. R. Devi and T. K. Maji, "Chemical modification of simul wood with styrene-acrylonitrile copolymer and organically modified nanoclay," *Wood Science and Technology*, vol. 46, no. 1–3, pp. 299–315, 2012.

[36] R. M. Rowell, "Chemical modification of wood: a short re-view," *Wood Material Science and Engineering*, vol. 1, no. 1, pp. 29–33, 2006.

[37] M. H. Schneider and K. I. Brebner, "Wood-polymer com-binations: the chemical modification of wood by alkoxysilane coupling agents," *Wood Science and Technology*, vol. 19, no. 1, pp. 67–73, 1985.

[38] J. J. Weiland and R. Guyonnet, "Study of chemical modifi-cations and fungi degradation of thermally modified wood using DRIFT spectroscopy," *Holz als Roh- und Werkstoff*, vol. 61, no. 3, pp. 216–220, 2003.

[39] I. Goñi, M. Gurruchaga, B. Vázquez, M. Valero, G. M. Guzmán, and J. S. Román, "Graft copolymerization of ethyl acrylate with alkyl methacrylates onto amylose initiated by cerium (IV). Microstructure of graft copolymers with respect to statistical copolymers," *Polymer*, vol. 35, no. 7, pp. 1535–1541, 1994.

[40] M. Gurruchaga, I. Goñi, M. Valero, and G. M. Guzmán, "Graft copolymerization of hydroxylic methacrylates and ethyl acrylate onto amylopectin," *Polymer*, vol. 33, no. 13, pp. 2860–2862, 1992.

[41] A. S. Singha and R. K. Rana, "Functionalization of cellulosic fibers by graft copolymerization of acrylonitrile and ethyl acrylate from their binary mixtures," *Carbohydrate Polymers*, vol. 87, no. 1, pp. 500–511, 2012.

[42] M. W. Sabaa, A. M. Elzanaty, O. F. Abdel-Gawad, and E. G. Arafa, "Synthesis, characterization and antimicrobial activity of schiff bases modified chitosan-graft-poly(acrylo-nitrile)," *International Journal of Biological Macromolecules*, vol. 109, pp. 1280–1291, 2018.

[43] T. Hajeeth, P. N. Sudha, K. Vijayalakshmi, and T. Gomathi, "Sorption studies on Cr (VI) removal from aqueous solution using cellulose grafted with acrylonitrile monomer,"

International Journal of Biological Macromolecules, vol. 66, pp. 295–301, 2014.

[44] G. Sharma, D. Pathania, M. Naushad, and N. C. Kothiyal, "Fabrication, characterization and antimicrobial activity of polyaniline Th(IV) tungstomolybdophosphate nanocomposite material: efficient removal of toxic metal ions from water," *Chemical Engineering Journal*, vol. 251, pp. 413–421, 2014.

[45] A. S. Singha, A. Guleria, and R. K. Rana, "Ascorbic acid/H_2O_2-initiated graft copolymerization of methyl methacrylate onto *Abelmoschus esculentus* fiber: a kinetic approach," *International Journal of Polymer Analysis and Characterization*, vol. 18, no. 1, pp. 1–14, 2013.

[46] K. B. Singh, J. Rajeev, and M. Mithu, "Induction of chemical and moisture resistance in *Saccharum spontaneum* L fiber through graft copolymerization with methyl methacrylate and study of morphological changes," *Journal of Applied Polymer Science*, vol. 113, no. 3, pp. 1781–1791, 2009.

[47] B. S. Rathore, G. Sharma, D. Pathania, and V. K. Gupta, "Synthesis, characterization and antibacterial activity of cellulose acetate-tin (IV) phosphate nanocomposite," *Carbohydrate Polymers*, vol. 103, pp. 221–227, 2014.

[48] M. Naushad, S. Vasudevan, G. Sharma, A. Kumar, and Z. A. Alothman, "Adsorption kinetics, isotherms, and thermodynamic studies for Hg^{2+} adsorption from aqueous medium using alizarin red-S-loaded amberlite IRA-400 resin," *Desalination and Water Treatment*, vol. 57, no. 39, pp. 18551–18559, 2016.

[49] G. Sharma, A. Kumar, M. Naushad et al., "Fabrication and characterization of gum Arabic-cl-poly(acrylamide) nanohydrogel for effective adsorption of crystal violet dye," *Carbohydrate Polymers*, vol. 202, pp. 444–453, 2018.

[50] F. A. Miller and C. H. Wilkins, "Infrared spectra and characteristic frequencies of inorganic ions," *Analytical Chemistry*, vol. 24, no. 8, pp. 1253–1294, 1952.

[51] G. Sharma, M. Naushad, A. A. H. Al-Muhtaseb et al., "Fabrication and characterization of chitosan-crosslinked-poly(alginic acid) nanohydrogel for adsorptive removal of Cr(VI) metal ion from aqueous medium," *International Journal of Biological Macromolecules*, vol. 95, pp. 484–493, 2017.

[52] A. M. Wróbel, M. Kryszewski, W. Rakowski, M. Okoniewski, and Z. Kubacki, "Effect of plasma treatment on surface structure and properties of polyester fabric," *Polymer*, vol. 19, no. 8, pp. 908–912, 1978.

[53] L. Segal, J. J. Creely, A. E. Martin, and C. M. Conrad, "An empirical method for estimating the degree of crystallinity of native cellulose using the X-ray diffractometer," *Textile Research Journal*, vol. 29, no. 10, pp. 786–794, 1959.

[54] V. Kumar, S. Naithani, and D. Pandey, "Optimization of reaction conditions for grafting of α-cellulose isolated from *Lantana camara* with acrylamide," *Carbohydrate Polymers*, vol. 86, no. 2, pp. 760–768, 2011.

[55] I. Kaur, R. Kumar, and N. Sharma, "A comparative study on the graft copolymerization of acrylic acid onto rayon fibre by a ceric ion redox system and a γ-radiation method," *Carbohydrate Research*, vol. 345, no. 15, pp. 2164–2173, 2010.

[56] I. Kaur, N. Sharma, and V. Kumari, "Modification of fiber properties through grafting of acrylonitrile to rayon by chemical and radiation methods," *Journal of Advanced Research*, vol. 4, no. 6, pp. 547–557, 2013.

[57] M. Naushad and Z. A. Alothman, "Separation of toxic Pb^{2+} metal from aqueous solution using strongly acidic cation-exchange resin: analytical applications for the removal of metal ions from pharmaceutical formulation," *Desalination and Water Treatment*, vol. 53, no. 8, pp. 2158–2166, 2015.